§17. Experimental Studies on the Neutron Emission Spectra and Activation Cross-Section in IFMIF Accelerator Structural Elements

Hagiwara, M., Baba, M., Uddin, M.S., Itoga, T., Hirabayashi, N., Oishi, T., Yamauchi, T. (Cylotron and Radioisotope Center, Tohoku Univ.), Sugimoto, M. (JAERI), Muroga, T.

To establish the database required for the design of IFMIF, we have been conducting systematic experiments on the neutron emission spectrum and radioactivity accumulation in IFMIF structural elements1). The experiments are carried out at the Tohoku University AVF cyclotron (K=110 MeV) facility equipped with a beam swinger system using the TOF method and a stack target method. In the previous reports, results on lithium for 25, 40 MeV deuterons were reported1).

Last year, we have carried out new experiments for 40 MeV deuterons and obtained new results for
1) neutron emission spectrum from a thick C, Al target and
2) activation cross-sections of the $^{nat}C(d,x)^{7}Be$, $^{27}Al(d,x)^{7}Be$, ^{22}Na, ^{24}Na reactions using a stacked target technique1).

The experimental method was almost the same with previous experiments1) and described only briefly here.

A deuteron beam from the Tohoku University cyclotron was transported to the target chamber at the center of the beam swinger system in the No.5 target room. The neutron spectrum was obtained by the TOF method using two NE213 scintillators, 14-cm-diam and 10-cm- thick, and 5-cm-diam and 5-cm-thick equipped with n- γ discriminators. The smaller one was employed for the measurement of low energy region. The data were accumulated as three-parameter data for TOF, n- γ spectra and pulse-height of the NE213 detector. The detection efficiency was obtained by calculation using the code SCINFUL-R.

The activities in the targets were measured after irradiation using high-pure Ge detectors by detecting the corresponding gamma-rays due to the decay of radioactive nuclides accumulated by the deuteron bombardment.

Thirty thin targets of carbon and aluminum with natural composition and 200-μm-thicknesses were prepared and stacked to stop the incident beam in the targets. The targets were set on a remotely-controlled target changer together with a beam viewer.

The beam current was around a few nano-amps or less. A Cu grid biased to -500 V was placed around the target for secondary electron suppression. The beam charge accumulated on the target was measured with an ORTEC current digitizer and a multi-channel scaler to record the time history of the beam.

Figures 1 and 2 show thick target neutron emission spectrum from carbon and aluminum, respectively, as a function of emission angle. Neutron spectra are observed over the almost entire range of secondary energies. The spectra for both elements show very similar feature and the difference is only in the maximum energy: The main peaks due to deuteron break-up reaction are observed around 15 MeV with very strong angular dependence similar with previous results for the Li(d,xn) reaction. This fact suggests that the breakup of incident deuterons is dominant in neutron emission. Such data are very few and will be useful for the model development of the neutron emission2).

In Fig.3-6, the results of the activation cross-sections are shown, together with other experiments and PHITS calculation. No other data are available for carbon. The present values for aluminum are consistent with other data but about two-times as large as the PHITS calculation. To estimate radioactivity induced by deuterons with PHITS, improvements will be required for cross-section calculation models2). The present experimental results will be used as the reference data to validate the Monte Carlo simulation and make shielding design of IFMIF.

Reference;

1) Aoki, T.,et al.: *J. Nuc. Sci. and Technol.*, Vol. 41, No. 4, p. 399 −405 (April 2004)
2)Hagiwara, M., et al.: J. Nucl. Materials, to be published

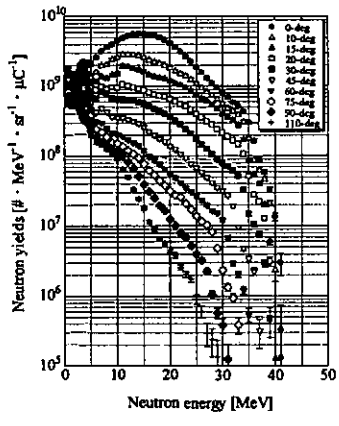

Fig.1 Thick target C(d,n) spectrum.

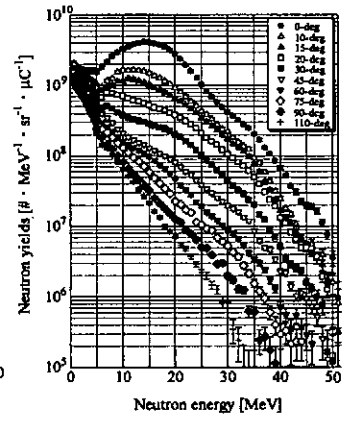

Fig.2 Thick target Al(d,n) spectrum.

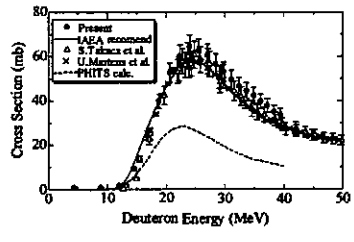

Fig.3 Al(d,x)^{24}Na cross-section

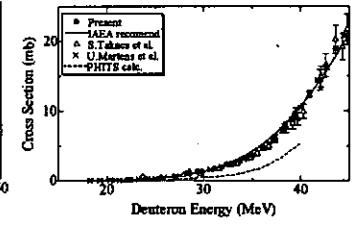

Fig.4 Al(d,x)^{22}Na cross-sections

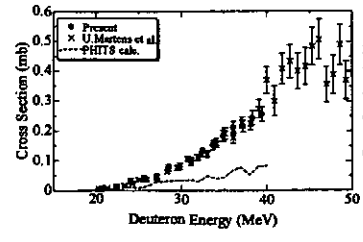

Fig.5 Al(d,x)^{7}Be cross-sections

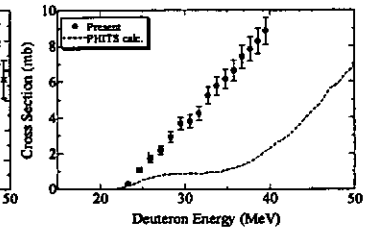

Fig.6 C(d,x)^{7}Be cross-sections